



OPEN

Comparison of [^{99m}Tc]Tc-FAPI SPECT/CT and [^{18}F]FDG PET/CT as predictive biomarkers for immunotherapy response in gastrointestinal cancer

Yu Zhang^{1,2,3,7}, Hong Chen^{3,4,7}, Dajia Lin^{3,4,7}, Zhiyi Lin^{1,2,3}, Jiyun Shi⁵, Hannan Gao⁵, Chenshen Huang^{3,4}, Fangqing Xue^{3,4}✉, Fan Wang⁶✉ & Wenxin Chen^{1,2,3}✉

To explore the diagnostic performance of [^{99m}Tc]Tc-FAPI SPECT/CT for gastrointestinal cancer, compared to [^{18}F]FDG PET/CT. In this analysis of a prospective trial, consecutively recruited patients from a single center with pathologically confirmed gastrointestinal cancer were prospectively enrolled from September 2022 to June 2024 and underwent paired v and [^{18}F]FDG PET/CT examinations at intervals of more than 1 day and within 7 days of each other. The activity of tracer accumulation in lesions was assessed by maximum standardized uptake value (SUV_{max}) and TBR (lesions SUV_{max} /ascending aorta SUV_{mean}). Histopathologic and clinical follow-up results were used as reference standards for final diagnoses. Seventy-eight patients (46 men; median age, 58.8 ± 14.5 years) were evaluated. Compared with the TBR for [^{18}F]FDG uptake, TBR for [^{99m}Tc]Tc-FAPI uptake was higher in primary tumor (4.6 ± 2.0 vs. 3.4 ± 1.7 ; $P = 0.001$), peritoneal spread (1.3 [$1.1, 7.3$] vs. 1.1 [$1.1, 1.1$]; $P = 0.001$) and liver metastases (2.5 [$1.1, 8.5$] vs. 1.1 [$1.1, 3.4$]; $P = 0.031$). For diagnostic accuracy in a total of 253 lesions in 78 patients, compared with [^{18}F]FDG PET/CT, [^{99m}Tc]Tc-FAPI SPECT/CT demonstrated a higher sensitivity (100% [15 of 15 lesions] vs. 20% [3 of 15]; $P < 0.001$), accuracy (100% [48 of 48 lesions] vs. 75% [36 of 48]; $P < 0.001$), and negative predictive value (100% [33 of 33 lesions] vs. 69% [36 of 48 lesions]; $P = 0.001$) in detecting peritoneal spread, and a higher sensitivity (85% [17 of 20 lesions] vs. 50% [10 of 20]; $P = 0.041$) in detecting liver metastases. Patients with metastatic gastrointestinal carcinomas negative on the [^{99m}Tc]Tc-FAPI scan showed improved clinical prognosis after immunotherapy ($P < 0.006$). TBR-FDG/TBR-FAPI was the main predictor of better prognosis post-immunotherapy ([stable disease, SD]+[partial response, PR]), with an optimal cut-off of 3.82. [^{99m}Tc]Tc-FAPI SPECT/CT can better evaluate peritoneal spread and liver metastases in gastrointestinal cancer. Furthermore, TBR-FDG/TBR-FAPI is a valuable imaging parameter for monitoring immunotherapy responses.

Keywords Gastrointestinal cancer, [^{99m}Tc]Tc-FAPI, SPECT/CT, Immunotherapy

Colorectal and gastric cancers, two types of gastrointestinal cancer, comprise 10.0% (ranked third) and 5.6% (ranked fourth) of all cancers, respectively¹. High incidence, high metastatic rate, high mortality, low early diagnosis, low radical resection, and low 5-year survival rates are typical features of gastrointestinal cancer^{2,3}. Owing to the lack of specific early signs and symptoms, many patients with gastrointestinal cancer present at an advanced stage. Early diagnosis and accurate staging are of utmost importance in determining the appropriate

¹Department of Nuclear Medicine, Fuzhou University Affiliated Provincial Hospital(Fujian Provincial Hospital), Fuzhou, China. ²Fujian Research Institute of Nuclear Medicine, Fuzhou, China. ³Shengli Clinical Medical College of Fujian Medical University, Fuzhou University Affiliated Provincial Hospital(Fujian Provincial Hospital), Fuzhou, China. ⁴Department of Gastrointestinal Surgery, Fuzhou University Affiliated Provincial Hospital(Fujian Provincial Hospital), Fuzhou, China. ⁵Key Laboratory of Biomacromolecules, CAS Center for Excellence in Biomacromolecules, Institute of Biophysics, Chinese Academy of Sciences, Beijing 100101, China. ⁶Medical Isotopes Research Center, Peking University, Beijing 100101, China. ⁷Yu Zhang, Hong Chen and Dajia Lin contributed equally to this work. ✉email: xuefangqingsl@sina.com; wangfan@bjmu.edu.cn; wenxinchzt@aliyun.com

treatment. [^{18}F]FDG PET/CT is extensively used for the diagnosis, staging, and preoperative evaluation of gastrointestinal malignancies. However, it has some limitations that are worth mentioning. Specifically, [^{18}F]FDG PET/CT has been found to have low sensitivity in the detection of primary gastrointestinal cancer, especially at an early stage, as well as for signet ring cells, mucinous cells, and poorly differentiated adenocarcinomas, which typically have a lower [^{18}F]FDG uptake. Moreover, peritoneal carcinomatosis is a common form of metastasis in gastrointestinal cancer and may have low sensitivity to [^{18}F]FDG PET. Therefore, it is necessary to develop more sensitive radioactive tracers for the diagnosis and staging of gastrointestinal tumors in order to contribute to personalized patient care. Fibroblast activation protein (FAP) is highly expressed in cancer-associated fibroblasts (CAFs) of various cancers, yet it is either not expressed or expressed at low levels in normal tissues, positioning it as a novel target for tumor imaging⁴. Numerous radioactive tracers utilizing FAP inhibitors (FAPI) have been developed for PET/CT imaging. [^{68}Ga]Ga-FAPI PET/CT has demonstrated good efficacy in the diagnosis, staging, and radiotherapy planning of gastrointestinal cancer^{5,6}. Moreover, it has higher detection sensitivity for primary and metastatic lesions of gastrointestinal tumors compared to [^{18}F]FDG PET/CT^{7,8}. Because of its low cost, single-photon emission computed tomography (SPECT)/CT using technetium-99m ($^{99\text{m}}\text{Tc}$) is widely available. [$^{99\text{m}}\text{Tc}$]Tc-FAPI offer attractive options for imaging in clinical situations where PET imaging is not accessible or is limited⁹. To date, research on the use of $^{99\text{m}}\text{Tc}$ -labelled FAPI has mainly focused on the optimization of [$^{99\text{m}}\text{Tc}$]Tc-FAPI synthesis¹⁰. However, to our knowledge, few studies have reported the potential advantages of [$^{99\text{m}}\text{Tc}$]Tc-FAPI SPECT/CT in gastrointestinal cancer staging and immunotherapy response.

Thus, the aim of this study was to explore the potential advantages of [$^{99\text{m}}\text{Tc}$]Tc-FAPI SPECT/CT in detecting metastatic lesions and immunotherapy response of gastrointestinal cancer in comparison with [^{18}F]FDG PET/CT, which is currently widely used.

Materials and methods

Patients

This prospective study was approved approved by the Ethics Committee of Fuzhou University Affiliated Provincial Hospital (No.K2022-09-016), and all methods were carried out following relevant guidelines and regulations. This study was carried out in compliance with the Declaration of Helsinki. Informed consent was obtained from all participants and/or their legal guardians. Between September 2022 and June 2024, 78 patients (46 men; median age, 58.8 ± 14.5 years) were recruited into this study. The key inclusion criteria were as follows: (1) histologically proven gastrointestinal adenocarcinoma (papillary, tubular, mucinous, signet ring cell, or poorly differentiated) by gastroscopy or surgery¹¹; (2) agreeing to perform both [$^{99\text{m}}\text{Tc}$]Tc-FAPI SPECT/CT and [^{18}F]FDG PET/CT and having signed a written informed consent; (3) [$^{99\text{m}}\text{Tc}$]Tc-FAPI SPECT/CT and [^{18}F]FDG PET/CT examinations at intervals of more than 1 day and within 7 days of each other; and (4) none of the patients received any antineoplastic therapy between the two scans. The exclusion criteria were as follows: (1) pregnancy or breastfeeding; (2) history of previous abdominal inflammatory diseases (such as peritonitis, pancreatitis, cholecystitis, inflammatory bowel disease); and (3) presence of a second primary tumor other than gastrointestinal adenocarcinoma. In this study, histopathologic examination of biopsy or resected surgical specimens served as the reference standard for the final diagnosis.

Radiopharmaceutical Preparation

The FAPI precursor [HYNIC-(PEG₄-OncoFAP)₂] was supplied by the Medical Isotopes Research Center, Peking University(Beijing, China) for research and development. [$^{99\text{m}}\text{Tc}$]TcO₄⁻ was procured from Guangdong CI Pharmaceutical Co., Fujian, China. For [$^{99\text{m}}\text{Tc}$]Tc-FAPI radiolabelling, 1 mL of 740–1369 MBq (20–37 mCi) of [$^{99\text{m}}\text{Tc}$]TcO₄⁻ saline solution was added to 25 μg of HYNIC-(PEG₄-OncoFAP)₂ and then incubated at 100°C for 20 min. [^{18}F]FDG was synthesized by our PET center using the MiniTrace accelerator and Microlab automatic synthesis system, both from GE, USA. The radiochemical purity of the final product exceeded 95%.

SPECT/CT imaging

For [$^{99\text{m}}\text{Tc}$]Tc-FAPI SPECT/CT, patients received an intravenous injection of 925 MBq (25 mCi) of [$^{99\text{m}}\text{Tc}$]Tc-FAPI. One hour post-injection, whole-body planar imaging and regional (neck-pelvic) SPECT/CT were conducted using the Discovery NM/CT 670Pro (GE, USA) equipped with low-energy, high-resolution collimators. The imaging protocol was as follows: for planar imaging, the peak energy was set at 140 keV, with a scan velocity of 15 cm/min in a 256×1025 matrix. For regional SPECT/CT: the camera matrix size was 128×128 ; zoom factor, 1.0; rotation, 360°; 30 s/frame over 60 frames. A low-dose CT protocol (130 keV, 60 mA) was utilized¹².

PET/CT imaging

For [^{18}F]FDG PET/CT, the patients fasted >6 h, and the blood glucose was monitored (<11.0 mmol/L) before the injection of [^{18}F]FDG (3.7MBq[0.1mCi]/Kg). [^{18}F]FDG PET/CT was performed 30 min after injection using a Discovery NM/CT 710(GE, USA). The image acquisition protocol was as follows: the CT scan was conducted with a tube voltage of 120 kV, an effective tube current of 110 mA, and a slice thickness of 3.75 mm. Immediately after the CT scan, a PET scan was performed in 3D acquisition mode (matrix: 200×200), with 6–8 bed positions for 2 min per position. The CT reconstruction data were utilized for attenuation correction on the PET images. Reconstructed data were processed using Bayesian penalized likelihood (BPL).

Imaging analysis

All images were independently analyzed by three experienced nuclear medicine physicians using a Xeleris Functional Imaging Workstation (Version 4.0; GE Healthcare). Differences in the determinations were discussed

until a consensus was reached. (1) Visual analysis: abnormally elevated [^{18}F]FDG or [$^{99\text{m}}\text{Tc}$]Tc-FAPI uptake was interpreted as positive if the possibility of physiological uptake, trauma, infection, or inflammation could be excluded. (2) Quantitative assessment: the region of interest around the positive lesion in the cross-sectional image was used to automatically calculate the maximum standard uptake value (SUV_{max}). The quantitative assessment was patient-based; if multiple metastatic lesions were present in one location, we calculated the average SUV_{max} , which represents the average SUV_{max} of all lesions ($n \leq 5$) or the average SUV_{max} of the five largest lesions ($n > 5$). The target-to-background ratio (TBR) was calculated by dividing the lesion SUV_{max} by the SUV_{mean} of the ascending aorta¹³.

Follow-up and verification

Histopathology of biopsy/resected surgical specimens served as the gold standard for the final diagnosis. When malignancy couldn't be determined, post-SPECT/CT scan surveillance data was sought. A disease was deemed malignant if any of the following was true: multi-modality imaging showed typical malignant features; follow-up imaging revealed marked size progression; or there was significant size reduction post -anticancer therapy. All suspected lesions underwent surveillance for a minimum of 6 months. All suspected lesions were followed up for no less than 6 months.

Immunohistochemistry (IHC) of FAP expression

FAP expression was analysed by IHC. Antigen retrieval was conducted using a heat - mediated approach with Tris/EDTA buffer (pH 9.0). Sections were incubated overnight at 4 °C with a 1:250 humanized anti-fibroblast activation protein antibody (Abcam, ab207178). Following this, they were treated with the labelled streptavidin-biotin (LSAB) complex. Finally, staining and visualization were performed using the iView DAB detection system (ZSGB-BIO, Beijing, China). Semiquantitative IHC analyses of FAP expression were performed by an experienced pathologist (score 0, no staining; score 1, 1–10% stromal staining; score 2, 10–50% stromal staining; score 3, 51–100% stromal staining).

Statistical analysis

Data analysis was performed using the SPSS software (version 19.0; IBM Corp., Armonk, NY, USA). Sankey plots were produced using the xiantao platform (www.xiantaozi.com). Normally distributed data were expressed as mean \pm SD, and nonnormally distributed data were expressed as median with IQR(interquartile range). The chi-square test was used to compare the differences in sensitivity, specificity, and accuracy of [$^{99\text{m}}\text{Tc}$]Tc-FAPI SPECT/CT and [^{18}F]FDG PET/CT. The McNemar χ^2 test was used to assess the differences in TBR between [$^{99\text{m}}\text{Tc}$]Tc-FAPI SPECT/CT and [^{18}F]FDG PET/CT. Kaplan-Meier survival curve analysis was used to compare the [^{18}F]FDG and [$^{99\text{m}}\text{Tc}$]Tc-FAPI scanning results (positive/negative) in assessing the therapeutic response to immunotherapy in patients with metastatic gastrointestinal cancer. Receiver operating characteristic (ROC) curve analysis was performed to evaluate the sensitivity, specificity, and cut-off value of the TBR-FDG/TBR-FAPI parameter. Two-tailed $P < 0.05$ was considered statistically significant.

Results

Participant characteristics

A schematic representation of the patient selection process is shown in Fig. 1. A total of 78 patients with gastrointestinal carcinomas confirmed by surgery or gastroscopy were enrolled in this study, including 33 patients with primary tumors for staging and 45 patients with the recurrent disease for restaging after surgery. Ten patients with primary tumors underwent surgery due to the early imaging stage. Sixty-eight patients with distant metastases received immunotherapy. Participant characteristics are listed in Table 1.

Diagnostic accuracy of [$^{99\text{m}}\text{Tc}$]Tc-FAPI SPECT/CT versus [^{18}F]FDG PET/CT

A total of 253 lesions in 78 patients were analyzed. The diagnostic accuracy of [$^{99\text{m}}\text{Tc}$]Tc-FAPI SPECT/CT for primary tumor and lymph node(LN) metastases were similar to that of [^{18}F]FDG PET/CT. However, for detecting the degree of peritonea spread, [$^{99\text{m}}\text{Tc}$]Tc-FAPI SPECT/CT had a sensitivity, accuracy and negative predictive value(NPV) of 100% (15 of 15), 100% (48 of 48) and 100% (33 of 33), respectively, and these values were higher than those for [^{18}F]FDG PET/CT (20% [3 of 15] [$P < 0.001$]; 75%[36 of 48] [$P < 0.001$]; and 69% [33 of 48] [$P = 0.001$], respectively); there were no evidence of a difference for specificity and positive predictive value(PPV). Meanwhile, [$^{99\text{m}}\text{Tc}$]Tc-FAPI SPECT/CT had a higher sensitivity for liver metastases than [^{18}F]FDG PET/CT (85% [17 of 20] vs. 50% [10 of 20] [$P = 0.041$]). For distant organ metastases in other sites(including bone, ovary, adrenal gland, lung and other distant organ metastases), [$^{99\text{m}}\text{Tc}$]Tc-FAPI SPECT/CT had a higher sensitivity and accuracy than [^{18}F]FDG PET/CT (100% [17 of 17] vs. 71% [12 of 17] [$P = 0.044$] and 100% [28 of 28] vs. 79% [22 of 28] [$P = 0.023$], respectively). The detailed data are presented in Table 2.

Comparison of [$^{99\text{m}}\text{Tc}$]Tc-FAPI and [^{18}F]FDG uptake in all lesions

As shown in Table 3; Fig. 2, the TBR for [$^{99\text{m}}\text{Tc}$]Tc-FAPI in primary tumor, peritoneal spread and liver metastases were higher than those for [^{18}F]FDG (4.6 ± 2.0 vs. 4.6 ± 2.0 [$P = 0.001$]; $1.3(1.1,7.3)$ vs $1.1(1.1,1.1)$ [$P = 0.001$] and $2.5(1.1,8.5)$ vs $1.1(1.1,3.4)$ [$P = 0.031$], respectively). No evidence of a difference in TBR was found between [$^{99\text{m}}\text{Tc}$]Tc-FAPI and [^{18}F] FDG in other metastases.

Immunohistochemistry analysis

A total of 10 primary tumor lesion specimens from 10 patients undergoing surgery were available. 70.0%(7/10) of primary tumor showed markedly positive FAP immunostaining (score 3); 20.0% (2/10) and 10.0%(1/10)

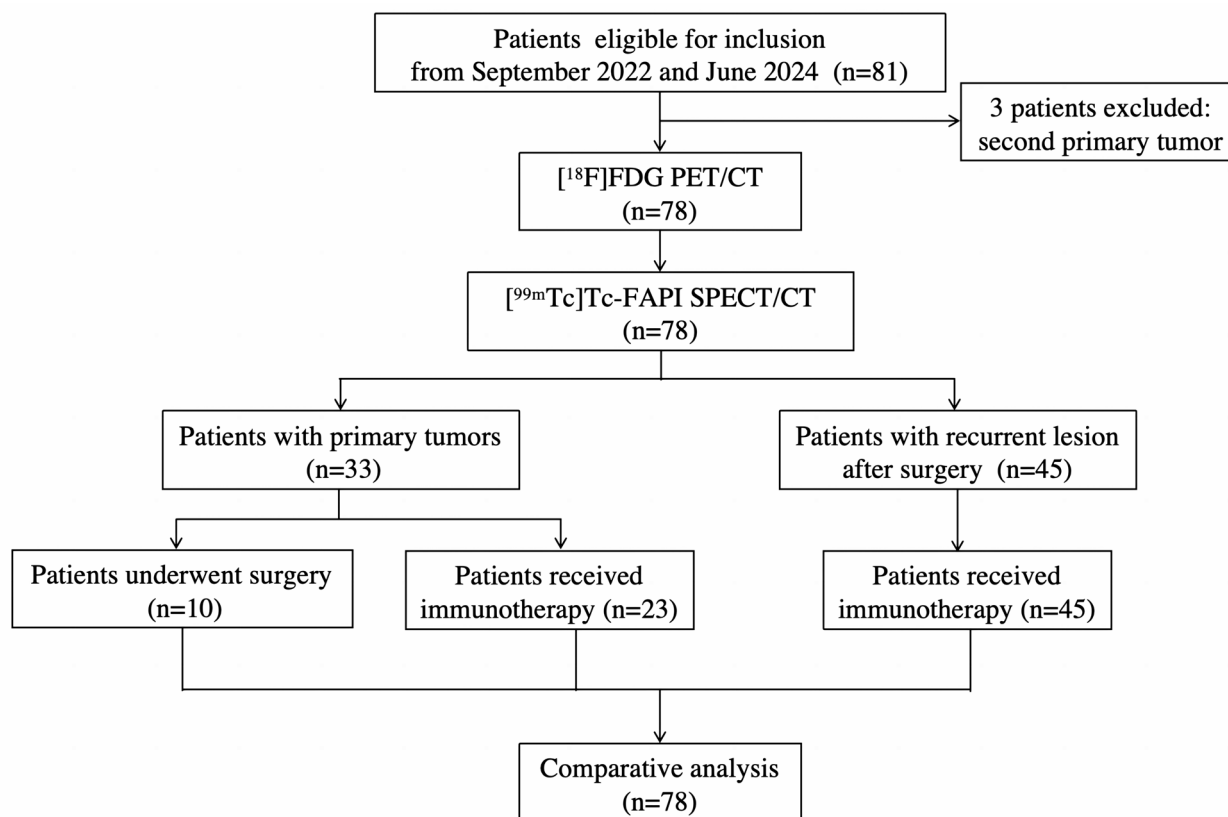


Fig. 1. Flow diagram shows the composition of enrolled patients. FAPI = fibroblast activation protein inhibitor, ^{18}F =fluorine 18, FDG = fluorodeoxyglucose.

Patient characteristic	Value
No. of patients	78
Age (years), median (range)	58.8 ± 14.5 (35–85)
Sex (Man/Woman)	46/32
Patient status, n (%)	
Staging	33 (42.3%)
Recurrence detection after surgery	45 (57.7%)
Diagnosis, n (%)	
Gastric cancer	40 (51.2%)
Colorectal cancer	38 (48.8%)
Site of disease, n	
Primary tumor	33
Lymph node	180
Peritoneal	15
Liver	20
Bone	1
Ovary	1
Adrenal gland	1
Lung	2
Total no. of lesions analyzed, n	253
Therapy modality, n (%)	
Surgery	10 (12.8%)
Immunotherapy	68 (87.2%)

Table 1. Participant characteristics. No=number.

Index	TP	FP	TN	FN	Sensitivity(%)	Specificity(%)	Accuracy(%)	PPV(%)	NPV(%)
Primary tumor									
¹⁸ F-FDG	33	0	0	0	100	... [†]	100	100	... [†]
^{99m} Tc-FAPI	33	0	0	0	100	... [†]	100	100	... [†]
LN metastases									
¹⁸ F-FDG	142	3	18	38	79(142/180)	86(18/21)	80(160/201)	98(142/145)	32(18/56)
^{99m} Tc-FAPI	127	0	21	53	71(127/180)	100(21/21)	74(148/201)	100(127/127)	28(21/74)
χ^2					3.309	3.231	1.999	2.657	0.215
<i>P</i> value					0.069	0.232	0.157	0.251	0.643
Peritonea metastases									
¹⁸ F-FDG	3	0	33	12	20(3/15)	100(33/33)	75(36/48)	100(3/3)	69(33/48)
^{99m} Tc-FAPI	15	0	33	0	100(15/15)	100(33/33)	100(48/48)	100(15/15)	100(33/33)
χ^2					20.000	... [†]	13.714	... [†]	10.400
<i>P</i> value					<0.001	... [†]	<0.001	... [†]	0.001
Liver metastases									
¹⁸ F-FDG	10	0	14	10	50(10/20)	100(14/14)	71(24/34)	100(10/10)	58(14/24)
^{99m} Tc-FAPI	17	0	14	3	85(17/20)	100(14/14)	91(31/34)	100(17/17)	82(14/17)
χ^2					5.584	... [†]	4.660	... [†]	2.651
<i>P</i> value					0.041	... [†]	0.062	... [†]	0.173
Metastases in other sites									
¹⁸ F-FDG	12	1	10	5	71(12/17)	91(10/11)	79(22/28)	92(12/13)	67(10/15)
^{99m} Tc-FAPI	17	0	11	0	100(17/17)	100(11/11)	100(28/28)	100(17/17)	100(11/11)
χ^2					5.862	1.048	6.720	1.353	4.540
<i>P</i> value					0.044	1.000	0.023	0.433	0.053

Table 2. Diagnostic accuracy of ^{99m}Tc-FAPI SPECT/CT and ¹⁸F-FDG PET/CT. ^{99m}Tc=Technetium-99m, FAPI = fibroblast activation protein inhibitor, ¹⁸F=fluorine 18, FDG = fluorodeoxyglucose, TP = true-positive, FP = false-positive, TN = true-negative, FN = false-negative, NPV = negative predictive value, PPV = positive predictive value. [†]Not calculable with the generalized linear model.

Site of Disease	TBR			
	^{99m} Tc-FAPI	¹⁸ F-FDG	Z value	P value
Primary tumor	4.6 ± 2.0	3.4 ± 1.7	3.620	0.001
Lymph node	1.7(0,6.0)	2.5(0,4.7)	-0.127	0.899
Peritoneal	1.3(1.1,7.3)	1.1(1.1,1.1)	-3.282	0.001
Liver	2.5(1.1,8.5)	1.1(1.1,3.4)	-2.151	0.031
Bone	4.0 ± 2.2	4.2 ± 2.7	-0.405	0.695
Ovary	5.8	5.6	... [†]	... [†]
Adrenal gland	4.1	4.9	... [†]	... [†]
Lung	2.5(2.3,4.0)	4.3(0,5.7)	0.000	1.000

Table 3. Comparison of ^{99m}Tc-FAPI and ¹⁸F-FDG uptake. FAPI = fibroblast activation protein inhibitor, ¹⁸F=fluorine 18, FDG = fluorodeoxyglucose, TBR = Tumor-to-Background Ratio. [†]Not calculable with the generalized linear model.

showed moderate (score 2) and slight (score 1) FAP immunostaining. Furthermore, the SUVmax of [^{99m}Tc]Tc-FAPI were moderately correlated with FAP expression ($r = 0.59$, $P = 0.023$).

Monitoring response to immunotherapy

FAP is highly expressed in tumor tissues yet it is either not expressed or expressed at low levels in non-tumor tissues⁴. Therefore, the degree of FAPI uptake as an imaging biomarker can exclude the influence of non-tumor related factors. To evaluate the potential of [^{99m}Tc]Tc-FAPI SPECT/CT imaging in predicting tumor responses to immunotherapy in patients with metastatic gastrointestinal carcinomas, we analyzed the progression free survival (PFS) of 68 patients with metastatic gastrointestinal carcinomas who received immunotherapy (PD-1 or PD-L1 blockade) after [^{99m}Tc]Tc-FAPI SPECT/CT and [¹⁸F]FDG PET/CT imaging in our clinical cohort. Kaplan-Meier curve demonstrated that patients with metastatic gastrointestinal carcinomas with [^{99m}Tc]Tc-FAPI SPECT/CT negativity had a better clinical prognosis after immunotherapy ($P < 0.001$) (Fig. 3). When the cut-off value for TBR-FDG/TBR-FAPI was set at 3.82, the sensitivity and specificity of better clinical prognosis

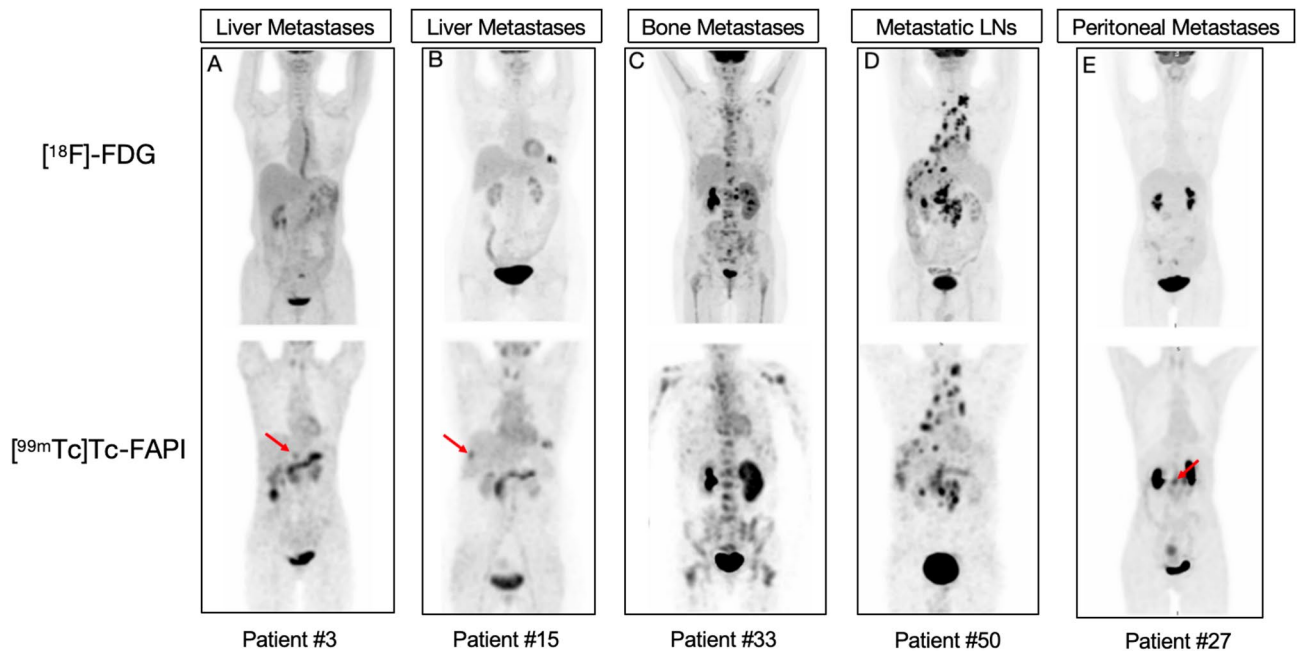


Fig. 2. (A–E) Representative $[^{18}\text{F}]$ FDG PET/CT and $[^{99\text{m}}\text{Tc}]$ Tc-FAPI SPECT/CT scans for five study patients with gastrointestinal cancer. $[^{18}\text{F}]$ FDG PET/CT and $[^{99\text{m}}\text{Tc}]$ Tc-FAPI SPECT/CT images show that uptake occurred in metastatic lymph nodes (LNs) (patient number 50, D) and bone metastases (patient number 33, C). $[^{99\text{m}}\text{Tc}]$ Tc-FAPI SPECT/CT outperformed $[^{18}\text{F}]$ FDG PET/CT in detecting liver metastases (patient number 3, A; and 15, B) and peritoneal spread metastases (patient number 27, E). Red arrows indicate foci additionally found by $[^{99\text{m}}\text{Tc}]$ Tc-FAPI SPECT/CT.

after immunotherapy ([stable disease, SD]+[partial response, PR]) were 68.3% (95% CI: 75.1–92.3%) and 100.0% (95% CI: 100.0–100.0%), respectively, with a Youden index of 0.748.

TNM staging based on $[^{99\text{m}}\text{Tc}]$ Tc-FAPI SPECT/CT compared with $[^{18}\text{F}]$ FDG PET/CT

Staging guidelines were based on the eighth edition of the TNM classification of malignant tumors of the Union for International Cancer. Figure 4 depicts changes in N and M staging of the gastrointestinal carcinomas in Sankey plots. Among 78 patients, 16 (20.5%) experienced a TNM change after $[^{99\text{m}}\text{Tc}]$ Tc-FAPI SPECT/CT. The most frequent reason for upstaging was the detection of new metastases on $[^{99\text{m}}\text{Tc}]$ Tc-FAPI SPECT/CT compared with $[^{18}\text{F}]$ FDG PET/CT (Fig. 5).

Discussion

FAP-targeted imaging is a new visualization imaging method for tumor stroma. In recent years, $[^{68}\text{Ga}]\text{Ga}$ -FAP PET imaging has been applied in digestive system cancers, with promising results^{8,14}. However, few reports have been published on SPECT/CT, a cost-effective imaging method, using $[^{99\text{m}}\text{Tc}]$ Tc-FAPI. PET generally provides superior spatial resolution and sensitivity compared to SPECT. Compared to FDG tracers, FAPI tracers have a lower background in normal liver and peritoneum, which leads to the potential use of FAPI tracers in patients with suspected liver and peritoneal metastases. Therefore, we intend to explore whether the different biological pathways of $[^{99\text{m}}\text{Tc}]$ Tc-FAPI tracer can compensate for the lack of spatial resolution and sensitivity in SPECT. To our knowledge, this is the first clinical experience with head-to-head comparison of $[^{99\text{m}}\text{Tc}]$ Tc-FAPI SPECT/CT and $[^{18}\text{F}]$ FDG PET/CT in digestive system cancers.

In our cohort study, $[^{99\text{m}}\text{Tc}]$ Tc-FAPI SPECT/CT and $[^{18}\text{F}]$ FDG PET/CT showed similar sensitivity for detection of digestive system cancers (100%), likely due to the predominance of stage T2 gastrointestinal cancers. Furthermore, $[^{99\text{m}}\text{Tc}]$ Tc-FAPI SPECT/CT showed a significantly higher TRB in primary lesions than did $[^{18}\text{F}]$ FDG PET/CT. The high TRB of $[^{99\text{m}}\text{Tc}]$ Tc-FAPI SPECT/CT for primary lesions may be attributed to the following factors: First, primary lesions in the stomach and intestines exhibit diffuse infiltrative growth, which is often accompanied by marked fibrosis¹⁵. Notably, approximately 40% of the tumor stroma in signet-ring cell carcinoma (SRCC) is enriched with CAFs, with CAFs comprising more than 50% of the tumor mass^{16,17}. Furthermore, previous studies have documented lower FDG uptake in SRCC and mucinous cancers compared to that in conventional adenocarcinomas, which is largely due to the relatively low expression levels of glucose transporter-1¹⁸. Therefore, SRCC demonstrated a higher uptake of FAPI, notably a higher TRB-FAPI. Furthermore, the physiological uptake of FAPI by the gastrointestinal tract is low, allowing for enhanced TRB-FAPI of primary lesions.

Accurate lymph node staging is very important for the clinical management of patients with gastrointestinal cancer, but conventional imaging scheme (CT or MR) has some limitations in evaluating lymph node

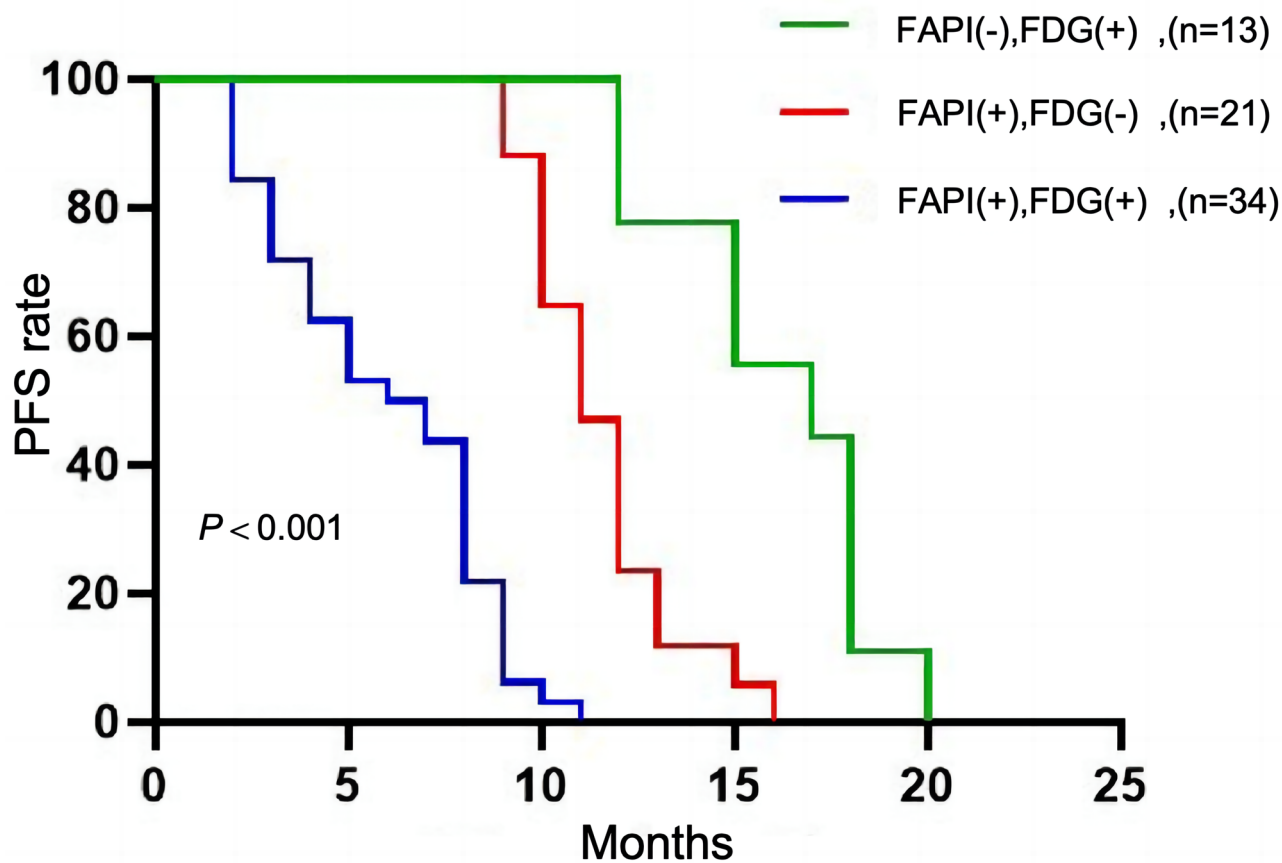


Fig. 3. Kaplan-Meier analysis of progression free survival (PFS) in 68 patients with metastatic gastrointestinal carcinomas with diferent [¹⁸F]FDG and [^{99m}Tc]Tc-FAPI scanning results.

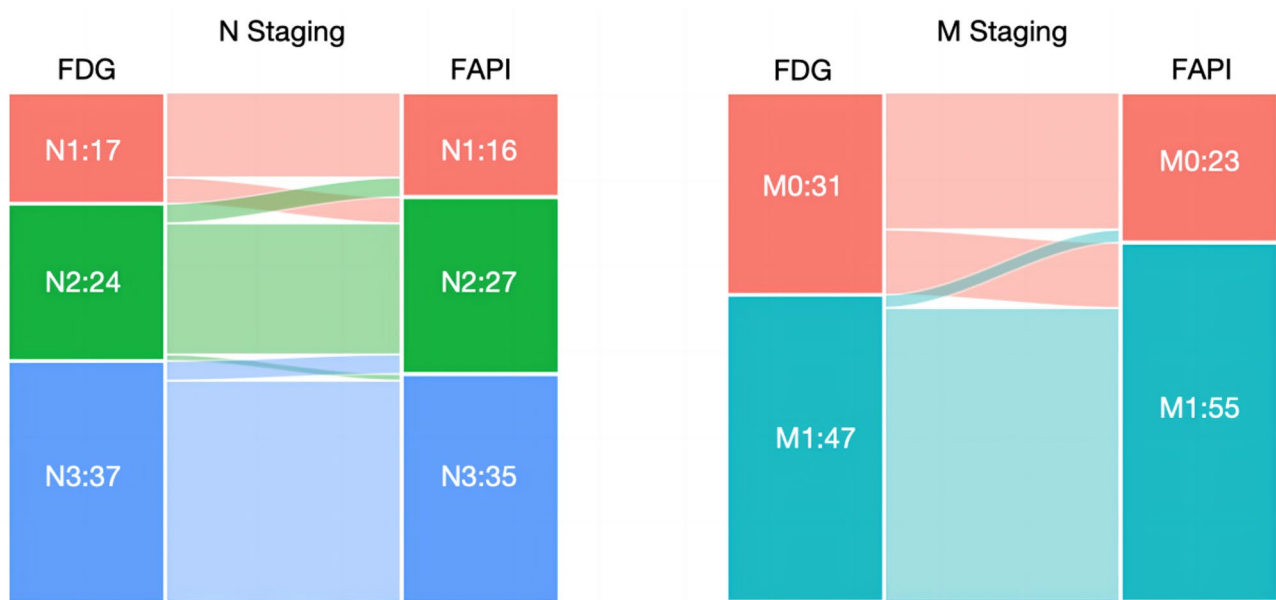


Fig. 4. Sankey plots displaying [^{99m}Tc]Tc-FAPI SPECT/CT and [¹⁸F]FDG PET/CT related changes in N and M staging of gastrointestinal cancer.

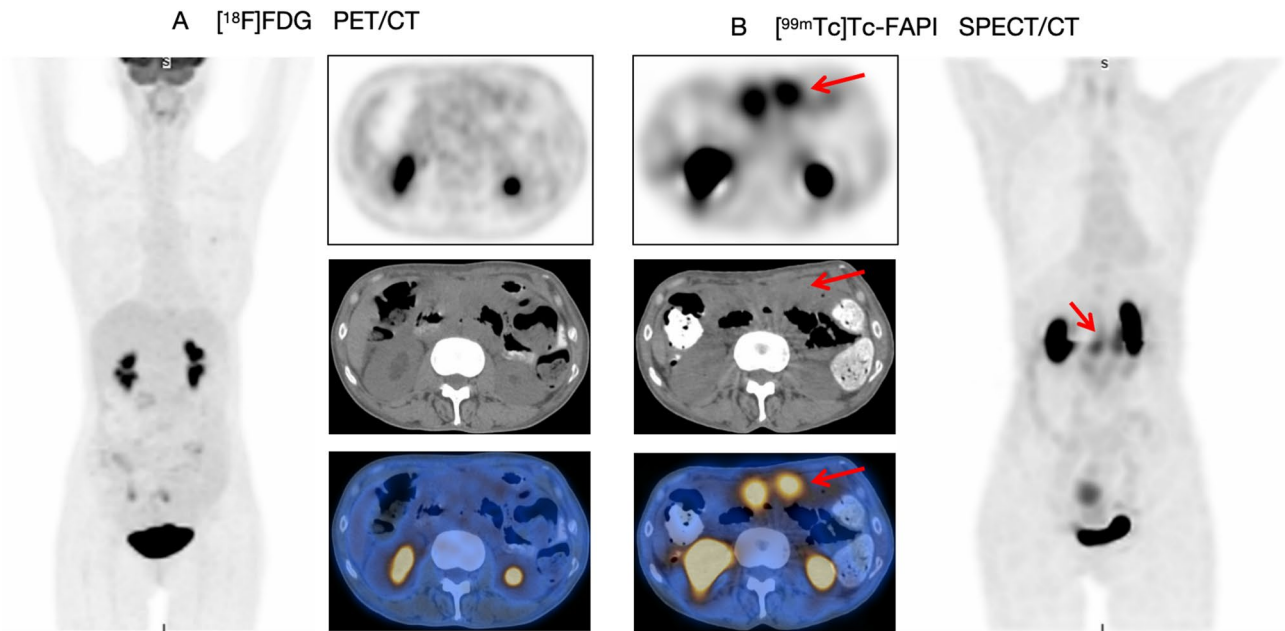


Fig. 5. An 63-year-old woman (patient number 27), confirmed a poorly cohesive gastric carcinoma by surgery, underwent $[^{18}\text{F}]\text{FDG}$ PET/CT and $[^{99\text{mTc}}]\text{Tc-FAPI}$ SPECT/CT scan to detect recurrence. $[^{99\text{mTc}}]\text{Tc-FAPI}$ SPECT/CT showed higher tracer uptake than $[^{18}\text{F}]\text{FDG}$ PET/CT (red arrow) for peritoneal carcinomatosis. Then, the ultrasound-guided abdominal puncture was performed, and the tumor cells were found in ascites, which confirmed the true-positive of $[^{99\text{mTc}}]\text{Tc-FAPI}$ SPECT/CT.

metastases^{19,20}. In lymph node analysis, Jia et al. found that $[^{99\text{mTc}}]\text{Tc-FAPI}$ SPECT/CT had a higher diagnostic accuracy than did enhanced CT for diagnosing lymph node metastases²¹. In our study, the diagnostic accuracy of $[^{99\text{mTc}}]\text{Tc-FAPI}$ SPECT/CT and $[^{18}\text{F}]\text{FDG}$ PET/CT in detecting metastatic lymph nodes was similar, diverging from previous $[^{68}\text{Ga}]\text{Ga-FAPI}$ PET/CT findings^{8,22}. We calculated that approximately 85% of the metastatic lymph nodes had diameters of ≤ 10 mm. The quantity of dissected lymph nodes was comparatively small. Due to its lower inherent resolution, SPECT/CT failed to detect many metastatic lymph nodes, which accounts for why $[^{99\text{mTc}}]\text{Tc-FAPI}$ SPECT/CT did not surpass $[^{18}\text{F}]\text{FDG}$ PET/CT in identifying metastatic lymph nodes.

Furthermore, gastrointestinal cancers are prone to distant metastases, notably to the lung, liver, bone, and peritoneum. Given the potential for radical treatment in patients with oligometastasis^{23,24}, early and precise evaluation of distant metastases is crucial for clinical management and treatment decisions. However, $[^{18}\text{F}]\text{FDG}$ PET/CT frequently fail to detect peritoneal metastases^{25,26}. In our research, $[^{99\text{mTc}}]\text{Tc-FAPI}$ SPECT/CT showed higher diagnostic accuracy than did $[^{18}\text{F}]\text{FDG}$ PET/CT for peritoneal metastases, and most metastases demonstrated a higher TBR on $[^{99\text{mTc}}]\text{Tc-FAPI}$ SPECT/CT. This may be attributed to the lack of physiological uptake of FAPI in the gastrointestinal tract, which is unaffected by the patient's blood glucose levels, thus enhancing the detection rate of peritoneal metastases. Concurrently, a pronounced fibrotic reaction occurs during peritoneal implantation and metastasis, leading to the upregulation of FAP expression in the lesions and consequently increasing FAPI uptake¹³. Notably, $[^{99\text{mTc}}]\text{Tc-FAPI}$ SPECT/CT also yielded false positives in the diagnosis of peritoneal metastases. According to previous $[^{68}\text{Ga}]\text{Ga-FAPI}$ PET/CT literature, postoperative fibrosis and/or inflammatory response, tuberculous peritonitis, hyperplasia of the omental fiber tissue, and other benign lesions can lead to increased FAPI uptake²⁷. Therefore, when clinically diagnosing peritoneal metastases, for $[^{99\text{mTc}}]\text{Tc-FAPI}$ avid lesions, combined with contemporaneous CT or MR anatomical imaging and the patient's clinical history, particularly past treatment history. This suggests that $[^{99\text{mTc}}]\text{Tc-FAPI}$ SPECT/CT is necessary in clinical practice for patients with peritoneal metastasis whose conventional imaging results are unclear. Additionally, our research discovers that $[^{99\text{mTc}}]\text{Tc-FAPI}$ SPECT/CT is inferior to $[^{18}\text{F}]\text{FDG}$ PET/CT in the M staging of gastrointestinal cancer. Significantly, we found the SUV_{max} -FAPI was moderately correlated with FAP expression. It can be explained by the fact that the determination of FAP expression was based on the randomly chosen regions of the tumor specimen, which was not a site-to-site hot-spot-to-pathological correlation. The quantitative index with SUV_{max} -FAPI may partly reflect the FAP expression.

Patients with metastatic gastrointestinal cancer exhibit a poor response to immunotherapy. Determining how to enhance the efficacy of immunotherapy and non-invasively identifying patients who are most likely to benefit remains a major clinical challenge in the treatment of gastrointestinal cancer. Moreover, the potential of $[^{99\text{mTc}}]\text{Tc-FAPI}$ SPECT/CT and $[^{18}\text{F}]\text{FDG}$ PET/CT in predicting or monitoring tumor response to immunotherapy is still largely unexplored. Recent studies indicate that CAFs play a pivotal role in resistance to tumor immunotherapy^{28,29}. Targeting FAP- α with $[^{99\text{mTc}}]\text{Tc-FAPI}$ SPECT/CT can facilitate the visualization of CAFs and, thus, the detection of tumor lesions. It has been observed that $[^{99\text{mTc}}]\text{Tc-FAPI}$ SPECT/CT outperforms $[^{18}\text{F}]\text{FDG}$ PET/CT in evaluating the response of metastatic gastrointestinal cancer to immunotherapy. Notably, a high

tumor uptake of [^{99m}Tc]Tc-FAPI is strongly associated with poor responses to immunotherapy. TBR-FDG/TBR-FAPI serves as the primary predictor of a favorable clinical prognosis following immunotherapy, with an optimal cutoff value established at 3.82. The observed phenomenon may be attributed to the fact that higher uptake of [^{99m}Tc]Tc-FAPI by tumor cells correlates with more active growth of fibroblasts around the tumor. These active fibroblasts then form a “physical barrier” encasing the tumor cells, thereby hindering the penetration of immunotherapy drugs into the tumor cells. Overall, our findings suggest that [^{99m}Tc]Tc-FAPI SPECT/CT imaging represents a promising non-invasive method for evaluating the response of metastatic gastrointestinal cancer to immunotherapy through the detection of CAFs in vivo.

The rapid advancement of PET technology, particularly the introduction of long-axial field-of-view PET scanners, has significantly improved the sensitivity and resolution of PET imaging³⁰. Compared to SPECT technology, PET offers higher sensitivity, resolution, and broader clinical applications, but it also has higher costs. With the introduction of FAPI-directed radioligand therapy (RLT) in tumour patients in recent years, interest in this field has increased. Targeted therapy can be effective only if the target protein is adequately expressed in most tumour lesions. Therefore, patients scheduled for ^{177}Lu -FAPI RLT should be screened by FAPI preimaging. Nevertheless, preimaging does not require the same high resolution as PET³¹. The choice between PET and SPECT depends on the specific clinical needs, availability of equipment, and considerations of cost-effectiveness.

Given the cost-effectiveness and availability of SPECT compared to PET, we believe that the following specific patient subgroups may benefit more from [^{99m}Tc]Tc-FAPI SPECT/CT: (1) patients with limited economic conditions or relatively scarce medical resources in their area; (2) Patients with peritoneal metastases; and (3) Radionuclides used in SPECT typically have a lower radiation dose, which is an important advantage for patients who require frequent tests or long-term monitoring.

The novelty of our study is characterized as follows: To our knowledge, this article represents the inaugural application of [^{99m}Tc]Tc-FAPI SPECT/CT for gastrointestinal cancer from a clinical viewpoint. First, this is the initial study to employ [^{18}F]FDG PET/CT as benchmarks for examining the benefits of [^{99m}Tc]Tc-FAPI SPECT/CT in assessing primary and metastatic lymph nodes as well as distant metastases of gastrointestinal cancer regarding sensitivity, specificity, and diagnostic accuracy. Second, it is the first investigation to analyze the association between primary lesion FAP expression and clinicopathological factors in gastrointestinal cancer. Finally, our study pioneers in determining whether [^{99m}Tc]Tc-FAPI SPECT/CT, a cost-effective imaging protocol, could potentially predict the prognosis of immunotherapy.

The findings of this study are significant; however, it also presented certain limitations. First, the research was conducted at a single center. Second, this cohort included a limited number of other parenchymal metastases, such as those in the ovaries, adrenal glands, and lungs, which precluded drawing definitive conclusions regarding the detection of these lesions. Moreover, most patients, who received immunotherapy, did not have biopsies of distant metastases performed. Instead, follow-up and additional imaging data, including MRI and CT, were utilized for definitive diagnoses. Therefore, our study does not establish a correlation between [^{99m}Tc]Tc-FAPI SPECT/CT imaging and immunohistochemistry of distant metastases.

In conclusion, [^{99m}Tc]Tc-FAPI SPECT/CT was found to be comparable to [^{18}F]FDG PET/CT in detecting primary lesions and lymph node metastases in patients with gastrointestinal tumors. Moreover, [^{99m}Tc]Tc-FAPI SPECT/CT demonstrated superior performance over [^{18}F]FDG PET/CT in detecting peritoneal involvement. Importantly, [^{99m}Tc]Tc-FAPI SPECT/CT imaging serves as a non-invasive tool for detecting CAFs, accurately reflecting tumor immunity, and can be utilized as an imaging biomarker to assess the therapeutic response to immunotherapy in patients with metastatic gastrointestinal cancer. Furthermore, TRB-FDG/TRB-FAPI is a promising molecular imaging parameter for predicting patient prognosis post-immunotherapy, which can help guide treatment planning for gastrointestinal cancer.

Data availability

The datasets used and/or analysed during the current study available from the corresponding author on reasonable request.

Received: 31 December 2024; Accepted: 7 May 2025

Published online: 14 May 2025

References

- Sung, H. et al. Global Cancer statistics 2020: GLOBOCAN estimates of incidence and mortality worldwide for 36 cancers in 185 countries. *CA Cancer J. Clin.* **71** (3), 209–249 (2021).
- Ajani, J. A. et al. Gastric cancer, version 2.2022, NCCN clinical practice guidelines in oncology. *J. Natl. Compr. Canc Netw.* **20** (2), 167–192 (2022).
- Benson, A. B. et al. Colon cancer, version 2.2021, NCCN clinical practice guidelines in oncology. *J. Natl. Compr. Canc Netw.* **19** (3), 329–359 (2021).
- Loktev, A. et al. A Tumor-Imaging method targeting Cancer-Associated fibroblasts. *J. Nucl. Med.* **59** (9), 1423–1429 (2018).
- Chen, H. et al. Comparison of [^{68}Ga]Ga-DOTA-FAPI-04 and [^{18}F] FDG PET/CT for the diagnosis of primary and metastatic lesions in patients with various types of cancer. *Eur. J. Nucl. Med. Mol. Imaging.* **47** (8), 1820–1832 (2020).
- Koerber, S. A. et al. The role of ^{68}Ga -FAPI PET/CT for patients with malignancies of the lower Gastrointestinal tract: first clinical experience. *J. Nucl. Med.* **61** (9), 1331–1336 (2020).
- Chen, H. et al. Usefulness of [^{68}Ga]Ga-DOTA-FAPI-04 PET/CT in patients presenting with inconclusive [^{18}F]FDG PET/CT findings. *Eur. J. Nucl. Med. Mol. Imaging.* **48** (1), 73–86 (2021).
- Pang, Y. et al. Comparison of ^{68}Ga -FAPI and [^{18}F]FDG uptake in gastric, duodenal, and colorectal cancers. *Radiology* **298** (2), 393–402 (2021).
- Lindner, T. et al. Design and development of ^{99m}Tc -Labeled FAPI tracers for SPECT imaging and ^{188}Re therapy. *J. Nucl. Med.* **61** (10), 1507–1513 (2020).

10. Ma, M. et al. Synthesis and preliminary study of ^{99m}Tc -Labeled HYNIC-FAPI for imaging of fibroblast activation proteins in tumors. *Mol. Pharm.* **21** (2), 735–744 (2024).
11. Amin, M. B. et al. *AJCC cancer Staging Manual* 8th edn (Springer, 2017).
12. Zhang, Y. et al. Improving diagnostic efficacy of primary prostate cancer with combined ^{99m}Tc -PSMA SPECT/CT and multiparametric-MRI and quantitative parameters. *Front. Oncol.* **13**, 1193370 (2023).
13. Qin, C. et al. ^{68}Ga -DOTA-FAPI-04 PET/MR in the evaluation of gastric carcinomas: comparison with ^{18}F FDG PET/CT. *J. Nucl. Med.* **63** (1), 81–88 (2022).
14. Liu, H., Yang, X., Liu, L., Qu, G. & Chen, Y. Comparison of ^{18}F FDG and ^{68}Ga -FAP-04 uptake in postoperative Re-evaluation of gastric, duodenal, and colorectal cancers. *Clin. Nucl. Med.* **48** (4), 304–308 (2023).
15. Erickson, L. A. Gastric Signet Ring Cell Carcinoma. *Mayo Clin Proc.* **92**(6):e95–e96. (2017).
16. Lee, D. et al. Intratumor stromal proportion predicts aggressive phenotype of gastric signet ring cell carcinomas. *Gastric Cancer.* **20** (4), 591–601 (2017).
17. Demuytere, J., Ceelen, W., Van Dorpe, J. & Hoorens, A. The role of the peritoneal microenvironment in the pathogenesis of colorectal peritoneal carcinomatosis. *Exp. Mol. Pathol.* **115**, 104442 (2020).
18. Choi, B. H. et al. Relation between Fluorodeoxyglucose uptake and glucose transporter-1 expression in gastric signet ring cell carcinoma. *Nucl. Med. Mol. Imaging.* **45** (1), 30–35 (2011).
19. Wang, J., Zhong, L., Zhou, X., Chen, D. & Li, R. Value of multiphase contrast-enhanced CT with three-dimensional reconstruction in detecting depth of infiltration, lymph node metastasis, and extramural vascular invasion of gastric cancer. *J. Gastrointest. Oncol.* **12** (4), 1351–1362 (2021).
20. Chen, W. B., Shi, Q. Q., Li, Z. M., Li, Z. Y. & Kang, L. Q. Diagnostic value of spiral CT energy spectrum imaging in lymph node metastasis of colorectal cancer. *Int. J. Colorectal Dis.* **37** (9), 2021–2029 (2022).
21. Jia, X. et al. The role of ^{99m}Tc -Tc-HFAPi SPECT/CT in patients with malignancies of digestive system: first clinical experience. *Eur. J. Nucl. Med. Mol. Imaging.* **50** (4), 1228–1239 (2023).
22. Lin, R. et al. ^{68}Ga [Ga-DOTA-FAPI-04 PET/CT in the evaluation of gastric cancer: comparison with ^{18}F FDG PET/CT. *Eur. J. Nucl. Med. Mol. Imaging.* **49** (8), 2960–2971 (2022).
23. Kinoshita, T. et al. Multicentre analysis of long-term outcome after surgical resection for gastric cancer liver metastases. *Br. J. Surg.* **102** (1), 102–107 (2015).
24. Han, Y. et al. Long-term outcome following microwave ablation of lung metastases from colorectal cancer. *Front. Oncol.* **12**, 943715 (2022).
25. Zhao, L., Pang, Y., Wei, J., Hao, B. & Chen, H. Use of ^{68}Ga -FAPi PET/CT for evaluation of peritoneal carcinomatosis before and after cytoreductive surgery. *Clin. Nucl. Med.* **46** (6), 491–493 (2021).
26. Panagiotopoulou, P. B., Courcousakis, N., Tentes, A. & Prassopoulos, P. CT imaging of peritoneal carcinomatosis with surgical correlation: a pictorial review. *Insights Imaging.* **12** (1), 168 (2021).
27. Alçın, G., Tatar, G., Şahin, R., Baloglu, M. C. & Çermik, T. F. Peritoneal tuberculosis mimicking peritoneal carcinomatosis on ^{68}Ga -FAPi-04 and ^{18}F -FDG PET/CT. *Clin. Nucl. Med.* **47** (8), e557–e558 (2022).
28. Kieffer, Y. et al. Single-Cell analysis reveals fibroblast clusters linked to immunotherapy resistance in Cancer. *Cancer Discov.* **10** (9), 1330–1351 (2020).
29. Khaliq, A. M. et al. Refining colorectal cancer classification and clinical stratification through a single-cell atlas. *Genome Biol.* **23** (1), 113 (2022).
30. Dimitrakopoulou-Strauss, A., Pan, L. & Sachpekidis, C. Long axial field of view (LAFOV) PET-CT: implementation in static and dynamic oncological studies. *Eur. J. Nucl. Med. Mol. Imaging.* **50** (11), 3354–3362 (2023).
31. Assadi, M. et al. Feasibility and therapeutic potential of ^{177}Lu -Fibroblast activation protein Inhibitor-46 for patients with relapsed or refractory cancers: A preliminary study. *Clin. Nucl. Med.* **46** (11), e523–e530 (2021).

Acknowledgements

The authors thank our Gastrointestinal Surgery colleagues, who referred the patients to our SPECT centre.

Author contributions

Guarantors of integrity of entire study, all authors; study concepts/study design or data acquisition or data analysis/interpretation, Y.Z., H.C.; manuscript drafting or manuscript revision for important intellectual content, Y.Z.; approval of final version of submitted manuscript, all authors; agrees to ensure any questions related to the work are appropriately resolved, all authors; literature research, Y.Z., H.C., Z.L.; clinical studies, all authors; statistical analysis, J.S., H.G., D.L., H.H.; and manuscript editing, F.X., F.W., W. C.

Funding

This study has received funding by the Joint Funds for National Natural Science Foundation of China (NSF-C, 2021Y9022), the Innovation of Science and Technology of Fujian Province (2021Y9022), Natural Science Foundation Youth Project of Fujian Province (2021J01221970), Joint Funds for the Innovation of Science and Technology, Fujian Province. (2023Y9299), Wu Jieping Medical Foundation Special Subsidy Fund for Clinical Research (320.6750.2023-03-41). The authors state that this work has not received any funding.

Declarations

Competing interests

The authors declare no competing interests.

Ethical approval

The studies involving human participants were reviewed and approved by Ethics Committee of Fuzhou University Affiliated Provincial Hospital (No.K2022-09-016).

Informed consent

Informed consent was obtained from all individual participants included in the study.

Additional information

Correspondence and requests for materials should be addressed to F.X., F.W. or W.C.

Reprints and permissions information is available at www.nature.com/reprints.

Publisher's note Springer Nature remains neutral with regard to jurisdictional claims in published maps and institutional affiliations.

Open Access This article is licensed under a Creative Commons Attribution-NonCommercial-NoDerivatives 4.0 International License, which permits any non-commercial use, sharing, distribution and reproduction in any medium or format, as long as you give appropriate credit to the original author(s) and the source, provide a link to the Creative Commons licence, and indicate if you modified the licensed material. You do not have permission under this licence to share adapted material derived from this article or parts of it. The images or other third party material in this article are included in the article's Creative Commons licence, unless indicated otherwise in a credit line to the material. If material is not included in the article's Creative Commons licence and your intended use is not permitted by statutory regulation or exceeds the permitted use, you will need to obtain permission directly from the copyright holder. To view a copy of this licence, visit <http://creativecommons.org/licenses/by-nc-nd/4.0/>.

© The Author(s) 2025